SUPPLEMENTAL MATERIAL

Expanded Materials & Methods

Animal model

All experimental protocols and surgical procedures were approved by Institutional Animal Care and Use Committee of The University of Texas MD Anderson Cancer Center and conformed to the National Institutes of Health guidelines for the ethical use of animals. No statistical methods were used to predetermine sample sizes for this study. However, our sample sizes were similar to those generally accepted in the field.[25, 31] Rats were randomly assigned to the control and treatment groups. Because CIH occurs similar in male and female patients,[1-3] we used male rats only in our study. The investigators were blinded during electrophysiological recordings and biochemical experiments. Male Sprague-Dawley rats (9–11 weeks old) were purchased from Envigo (Indianapolis, IN) and housed in the animal facility at a controlled temperature (25 ± 1°C) and lighting (12-h light/dark cycles). All animals had free access to rodent food and tap water. FK506 (#3631, Tocris Bioscience) was dissolved in dimethyl sulfoxide at a concentration of 30 mg/mL and injected intraperitoneally at a dose of 3 mg/kg once a day for 14 consecutive days. Rats received vehicle (dimethyl sulfoxide) injection for 14 days were used as a control group. Final biochemical and electrophysiological experiments were performed 7 days after the last treatment of FK506. Memantine (#14184, Cayman Chemical) was administered via intraperitoneal injection or in the drinking water.

Arterial blood pressure measurement with radiotelemetry

ABP was measured in free-moving rats using a Millar telemetry system (Telemetry Research Ltd).[13, 27] Briefly, rats were anesthetized with 2–3% isoflurane, and a catheter of telemetry transmitter was inserted into the descending aorta. The transmitter was implanted in the abdominal cavity. After surgery, rats were housed individually and received subcutaneous injection of buprenorphine (0.5 mg/kg, every 12 h for 2 days) and enrofloxacin (5 mg/kg, daily for 3 days). Rats were allowed to recover for two weeks after surgery and then received FK506 or DMSO treatment. ABP data in free-moving rats were recorded continuously and analyzed using a data acquisition system (LabChart 7, AD Instruments). Heart rate (HR) values were derived from the blood pressure pulse signal.

Calcineurin activity measurement

Calcineurin activity in brain tissues was measured using a calcineurin cellular activity assay kit (#207007, Millipore).[32] Briefly, fresh brain samples, including the hypothalamus, PVN, frontal cortex, hippocampus, organum vasculosum laminae terminalis (OVLT), subfornical organ (SFO), and RVLM, were obtained from FK506-treated and vehicle-treated rats. We pooled PVN and SFO tissues from 2 rats in each sample. Tissues were homogenized in lysis buffer containing 50 mM Tris, 1 mM DTT, 100 μM EDTA, 100 μM EGTA, 0.2% Nonidet P-40, and a protease inhibitor cocktail (pH, 7.4). Then, the samples were centrifuged at 200,000*g* for 45 min at 4°C, and the resulting supernatant was passed through desalting column resin to remove excess phosphate and nucleotides.

Calcineurin activity was determined by using RII phosphopeptide substrate supplied with the kit, and free phosphate release was detected based on malachite green assay at 620 nm. Calcineurin activity was calculated as the difference of free phosphate release between assays with and without EGTA. Assay for each sample were performed in duplicate. Calcineurin activity was expressed per μg protein for each reaction and normalized to the vehicle group.[33]

Synaptosome isolation and immunoprecipitation

Synaptosomes were isolated from the brain in rats as described previously.[31, 34] Under anesthesia induced by 2–3% isoflurane, rats were decapitated, and their brains were quickly removed and placed in an ice-cold artificial cerebrospinal fluid (aCSF) saturated with 95% O_2 and 5% CO_2. The aCSF contained (in mM) 126 NaCl, 3 KCl, 1.5 $MgCl_2$, 2.4 $CaCl_2$, 1.2 NaH_2PO_4, 11.0 glucose, and 26.0 $NaHCO_3$ (300–310 mOsmol/L). Hypothalamic slices were sectioned at 1.08–2.12 mm caudal to the bregma, and PVN and RVLM samples were micropunched bilaterally with a slice punch (0.5 mm diameter) according to their respective stereotactic co-ordinates.[30, 34, 35] To isolate synaptosomes, we homogenized the tissues (pooled from 2 rats for each sample) using 10 volumes of ice-cold HEPES-buffered sucrose, which contained (in mM) 0.32 sucrose, 1 EGTA, 4 HEPES (pH, 7.4), and a protease/phosphatase inhibitor cocktail (#78442, Thermo Scientific). The homogenate was initially centrifuged at 2,000*g* for 10 min at 4°C to remove the nuclei and large debris and was followed by centrifugation at 20,000*g* for 30 min to obtain the crude synaptosomal fraction. The synaptosomal pellet was then lysed via hypo-osmotic shock in 9 volumes of ice-cold HEPES-buffer with protease inhibitor cocktail (#P8340, Sigma-Aldrich) for 30 min. The lysate was centrifuged at 25,000*g* for 45 min at 4°C to obtain synaptosomal membrane fraction, which was dissolved in sodium dodecyl sulfate sample buffer at a final concentration of 0.25 μg/μl. The protein concentration in the sample was quantified using a Bradford protein assay (#5000201, Bio-Rad).

Synaptosomal samples were incubated at 4°C overnight with Protein G beads (#16-266, EMD Millipore) prebound to rabbit anti-phosphoserine (#AB1603, Millipore) or rabbit anti-phosphothreonine antibodies (#AB1607, Millipore). Protein G beads prebound to rabbit IgG were used as controls. Samples were washed three times with immunoprecipitation buffer containing 50 mM Tris (pH, 7.4), 250 mM NaCl, 0.5% NP-40, and a protease inhibitor cocktail (#P8340, Sigma-Aldrich). Proteins were separated by running in 4%–12% Bis-Tris grade gels (#NP0335BOX, Invitrogen). Then, the samples were immunoblotted with a mouse anti-GluN1 antibody (1:500; #75-272, NeuroMab), mouse anti-GluN2A antibody (1:500; #75-288; NeuroMab), and mouse anti-GluN2B antibody (1:500; #75-097, NeuroMab). The specificity of primary antibodies has been shown previously.[31, 36] The blotting membranes were incubated with an HRP–conjugated anti-mouse antibody (1:2000; #ab97023, Abcam). The protein bands were detected and quantified using an Odyssey Fc Imager (LI-COR Biosciences) and normalized by the respective input bands in the same blot.

Immunocytochemical staining of PVN presympathetic neurons

Spinally projecting PVN neurons were retrogradely labeled with Alexa Fluor 594-conjugated cholera toxin subunit-B (CTB; #C34777, ThermoFisher Scientific) injected to the intermediolateral cell column of the thoracic spinal cord, as described previously.[29, 37] Rats were deeply anesthetized with sodium pentobarbital (60 mg/kg, intraperitoneally) and intracardially perfused with 4% paraformaldehyde 7 days after CTB injection. Coronal brain sections (30 μm thick) containing the PVN were blocked with 5% goat serum for 1 h at 22°C and incubated overnight with a primary rabbit anti-calcineurin antibody (1:500; #07-1490, Millipore), which recognizes both the catalytic A and regulatory B subunits of calcineurin. Tissue sections incubated with the secondary antibody only were included and used as a control. The sections were then incubated with an Alexa Fluor 488–conjugated goat anti-rabbit secondary antibody (1:1000; #ab150077, Abcam) for 2 h at 22°C. After rinsing, the sections were mounted on slides, dried, and coverslipped. The sections were viewed under a confocal microscope (model LSM510, Carl Zeiss Microscopy, NY), and areas of interest were photographed.

Electrophysiological recording of PVN presympathetic neurons in brain slices

Spinally projecting and RVLM-projecting PVN neurons were retrogradely labeled as described previously.[30, 38] In brief, rats were anesthetized using 2–3% isoflurane, and the spinal cord at T2 to T4 levels was exposed via laminectomy. FluoSpheres (0.04 μm, Invitrogen) were pressure injected through a glass pipette (tip, 20–30 μm) into the intermediolateral region of the spinal cord in 3 separate 50-nL injections on each side. To label RVLM-projecting neurons in the PVN, FluoSpheres were microinjected into the RVLM in accordance with the stereotactic co-ordinates: 12.5–13.0 mm caudal to the bregma, 1.9–2.0 mm lateral to the midline, and 7.5–8.0 mm ventral to the dura.[30, 31] After injection, rats received subcutaneous injection of buprenorphine (0.5 mg/kg, every 12 h for 2 days) and enrofloxacin (5 mg/kg, daily for 3 days). Rats were allowed to recover for 7 days to permit FluoSpheres to be retrogradely transported to the PVN. FluoSphere-injected animals were anesthetized with 3% isoflurane and decapitated. The brain was quickly removed and placed in the ice-cold aCSF continuously gassed with a mixture of 95% O_2 and 5% CO_2. A tissue block containing the hypothalamus was cut from the brain and glued onto the stage of a vibratome (VT1000, Leica Biosystems Inc.). Coronal hypothalamic slices containing the PVN were sectioned (300 μm thick) and pre-incubated in aCSF gassed with a mixture of 95% O_2 and 5% CO_2 at 34°C for at least 1 h before recording. The brain slices were then transferred to a glass-bottom chamber and perfused with aCSF at 3.0 ml/min at 34°C maintained by an inline solution heater and temperature controller.

Fluorescence-labeled neurons are predominantly located in the medial one-third (the mediocellular region) of the PVN, which is between the third ventricle and the fornix.[27, 39, 40] These labeled neurons in the PVN were visually identified on an upright microscope equipped with epifluorescence illumination and differential interference contrast optics. The firing activity of labeled PVN neurons was recorded using a perforated whole-cell method, as we described previously.[41, 42] The recording electrode was pulled from borosilicate capillaries (1.2-mm OD, 0.68-mm ID; World Precision Instruments) using a micropipette puller. The perforated recording keeps stable intracellular environment and minimizes run-down during the recording. The internal solution in the recording

pipette contained (in mM) 130.0 K-acetate, 15.0 KCl, 5.0 NaCl, 1.0 $MgCl_2$, and 10.0 4-(2-hydroxyethyl)-1-piperazineethanesulfonic acid (HEPES) (pH adjusted to 7.2 with 1 M KOH; 290–300 mOsmol/L). Gramicidin was dissolved in DMSO and diluted in the internal solution to a final concentration of 50 μg/mL. We started to record the firing activity of labeled PVN neurons when the firing rate had reached a steady state with resting membrane potentials at –50 mV or lower and with action potential overshoots of more than 10 mV.[41-43]

The miniature excitatory postsynaptic currents (mEPSCs) were recorded using whole-cell voltage-clamp at a holding potential of –60 mV in the presence of 1 μM tetrodotoxin and 20 μM bicuculline.[31] The internal solution contained (in mM) 135.0 K-gluconate, 5.0 tetraethylammonium, 2.0 $MgCl_2$, 0.5 $CaCl_2$, 5.0 HEPES, 5.0 ethylene glycol tetraacetic acid (EGTA), 5.0 Mg-ATP, 0.5 Na-GTP, and 10 lidocaine N-ethyl bromide (pH adjusted to 7.2 with 1 M KOH; 290–300 mOsmol/L). The postsynaptic α-amino-3-hydroxy-5-methyl-4-isoxazolepropionic acid receptor (AMPAR)- and NMDAR-currents were elicited by puff application of AMPA (100 μM) or NMDA (100 μM) directly to the recorded PVN neuron at a holding potential of –60 mV in the presence of 1 μM tetrodotoxin, as we described previously.[26, 29] The puff pipette (tip diameter ~10 μm) was placed about 150 μm away from the recorded neuron, and NMDA or AMPA solution was ejected using a Pressure System IIe (4 psi, 50 ms; Toohey Company). Because NMDAR is blocked by Mg^{2+} at a negative holding potential and co-activated by glycine, puff NMDA–elicited currents were recorded in Mg^{2+}-free aCSF in the presence of 10 μM glycine.[26, 31] All the signals were processed using a MultiClamp 700B amplifier (Molecular Devices), filtered at 1–2 kHz, digitized at 20 kHz using DigiData 1320A (Molecular Devices), and saved to the hard drive of a computer. Tetrodotoxin (#HB1035), 2-amino-5-phosphonopentanoic acid (AP5, #HB0252), and 6-cyano-7-nitroquinoxaline-2,3-dione (CNQX, #HB0204) were purchased from Hello Bio Inc.

PVN microinjection and recording of renal sympathetic nerve activity *in vivo*.

Rats were anesthetized by intraperitoneal injection of a mixture of α-chloralose (60 mg/kg) and urethane (800 mg/kg). Rats were mechanically ventilated through a trachea cannula connected to a rodent ventilator. The concentration of CO_2 in the expiration was monitored by a CO_2 analyzer (model CapStar-100, CWE) and maintained at 4% to 5% by adjusting respiratory rate (~60 bpm) and tidal volume (~2.5 mL) throughout the experiment. ABP was monitored through a cannula inserted into the left femoral artery, and HR was derived from pulsatile blood pressure signal. A retroperitoneal incision was made, and a branch of the left renal postganglionic sympathetic nerve was isolated under a surgical microscope. Renal nerve was cut distally to ensure that afferent nerve activity was not recorded.[25, 35] The central end of the renal nerve was placed on a bipolar stainless steel recording electrode, and the renal sympathetic nerve activity (RSNA) was amplified (gain, 20,000–30,000) and filtered (band-pass, 100–3000 Hz) using an alternating-current amplifier (model P511, Grass Instrument) and monitored using an audio amplifier (Grass Instrument). The RSNA and ABP signals were recorded using a 140-PLUS analog-to-digital and Spike2 system (Cambridge Electronic Design).

A microinjection pipette (tip diameter 20–30 μm) was advanced into the PVN in accordance with the stereotactic co-ordinates: 1.6–2.0 mm caudal to the bregma, 0.5 mm lateral to the midline, and 7.0–7.5 mm ventral to the dura.[25, 31] The microinjection was performed using a Nanoject II injector (Drummond Scientific Company) and monitored under a surgical microscope. The basal level of RSNA after subtraction of background noise was set as 100%, and the percent change in RSNA from the baseline value was calculated.

Statistical analysis

All data were presented as means ± SEM. The animals were assigned using a simple randomization method (1:1 allocation) to the control and treatment groups, and no animals were excluded from the study. ABP and HR were averaged during light and dark cycles, and mean ABP was calculated with a standard formula (diastolic ABP + 1/3 [systolic ABP – diastolic ABP]). The raw RSNA was integrated with an interval of 1.0 s using Spike2 software after background noise was subtracted.[25, 44] The junction potentials in whole-cell recordings were corrected off-line based on the composition of internal and external solution used. The firing rate and mEPSCs were analyzed over a period of 3–6 min before, during, and after drug application using a peak detection program (MiniAnalysis, Synaptosoft). The difference of cumulative probability of amplitudes and inter-event intervals of mEPSCs were determined using Kolmogorov–Smirnov test. The amplitude of currents elicited by puff NMDA and AMPA application was calculated by averaging three consecutive current traces. No test for outlier in the data was conducted, and all data sets in the present study were normally distributed, assessed using the Shapiro–Wilk test. Two-tailed Student's *t* test was used to determine differences between two groups. Repeated measures ANOVA followed by Dunnett's *post hoc* test or two-way ANOVA followed by Bonferroni's *post hoc* test was used to determine differences among three or more groups. All statistical analyses were performed using Prism software (version 8, GraphPad). $p < 0.05$ was considered statistically significant.

Online Figures

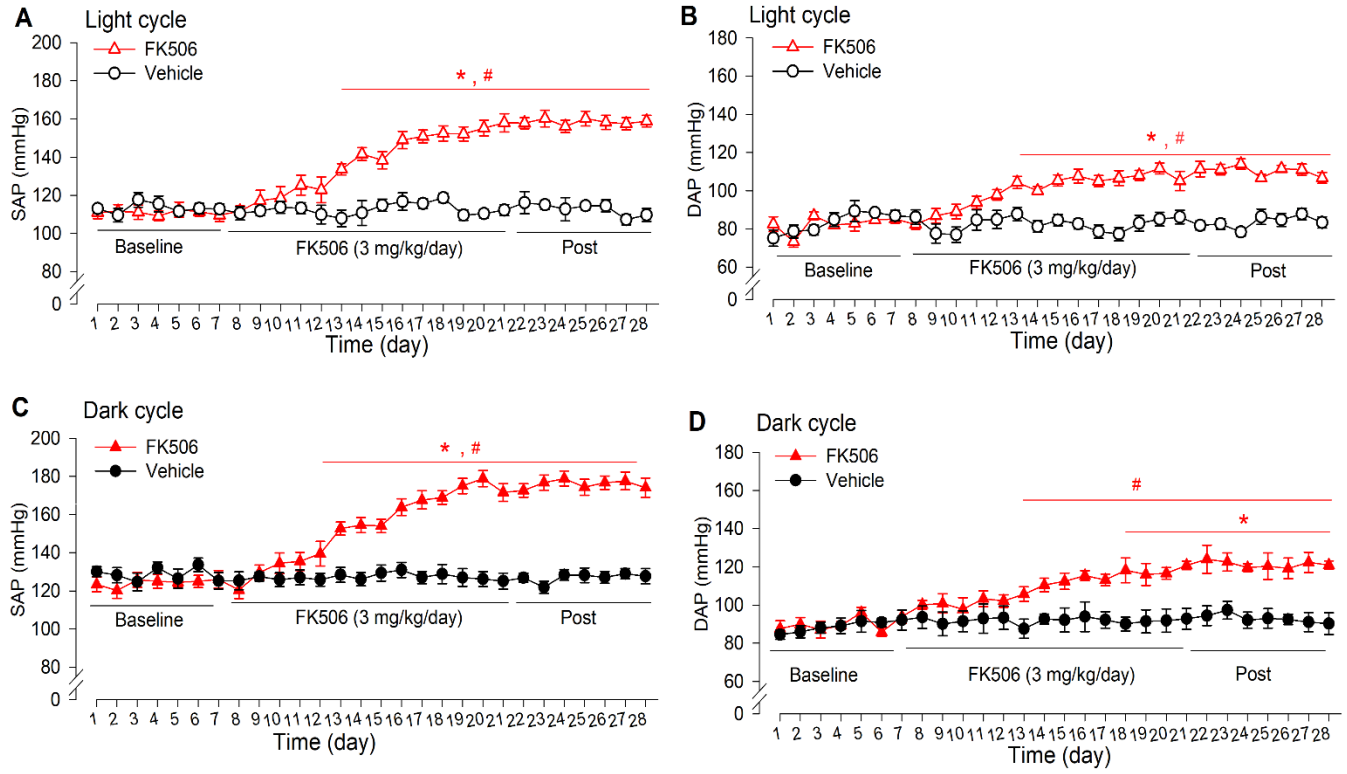

Figure S1. Changes in systolic and diastolic ABP in rats treated with FK506 or vehicle. **A-D**, Time course of changes in systolic (SAP) and diastolic ABP (DAP) in light (**A** and **B**) and dark (**C** and **D**) cycles recorded using radiotelemetry in conscious rats treated with FK506 (3 mg/kg/day) or vehicle for 14 days (n = 6 rats per group). Telemetry data were averaged during the light (7:00 A.M. to 7:00 P.M.) and dark period (7:00 P.M. to 7:00 A.M. the next day) each day. *$p < 0.05$ compared with the respective values at the same time point in the vehicle group; $^{\#}p < 0.05$ compared with the baseline within the group (two-way ANOVA followed by Bonferroni's *post hoc* test). Exact p values are shown in **Tables 3-1** and **3-2**.

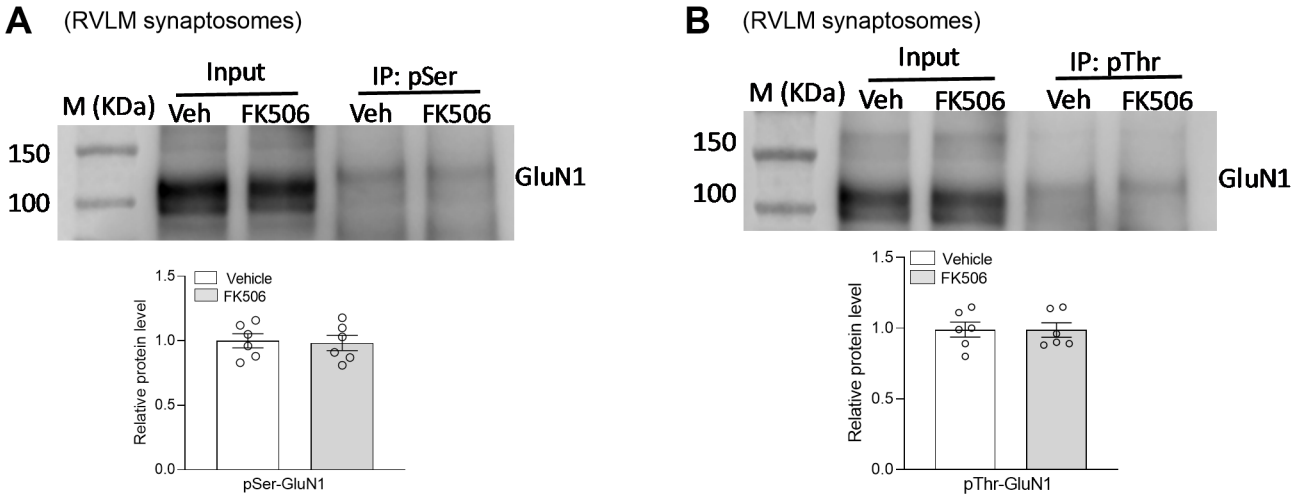

Figure S2. Systemic treatment with FK506 has no effect on NMDAR phosphorylation in the RVLM. **A** and **B**, Representative blotting images and quantification show the protein levels of phosphoserine (pSer)-GluN1 (**A**) and phosphothreonine (pThr)-GluN1 (**B**) in RVLM synaptosomes obtained from rats 7 days after terminating treatment with FK506 or vehicle (Veh). IP, immunoprecipitation. Data are expressed as mean ± SEM (n = 6 rats per group).

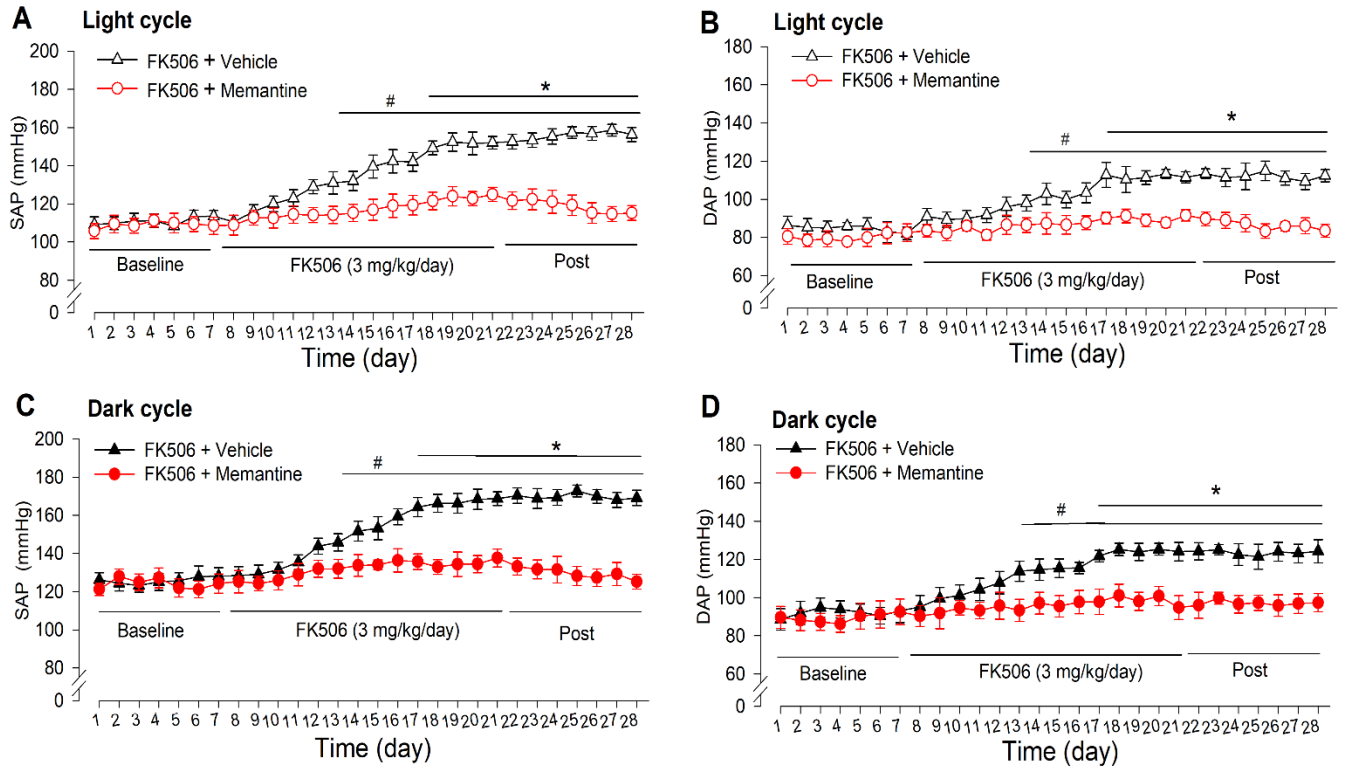

Figure S3. Changes in systolic and diastolic ABP in rats concurrently treated with FK506 and memantine. **A-D**, Time course of changes in systolic (SAP) and diastolic ABP (DAP) in light (**A** and **B**) and dark (**C** and **D**) cycles recorded using radiotelemetry in conscious rats concurrently treated with FK506 (3 mg/kg/day) and memantine (20 mg/kg/day in the drinking water) or vehicle for 14 days (n = 6 rats per group). Telemetry data were averaged during the light (7:00 A.M. to 7:00 P.M.) and dark (7:00 P.M. to 7:00 A.M. the next day) period each day. $^{*}p < 0.05$ compared with the respective values at the same time point in the vehicle group; $^{\#}p < 0.05$ compared with the baseline within the group (two-way ANOVA followed by Bonferroni's *post hoc* test). Exact p values are shown in **Tables 4-1** and **4-2**.

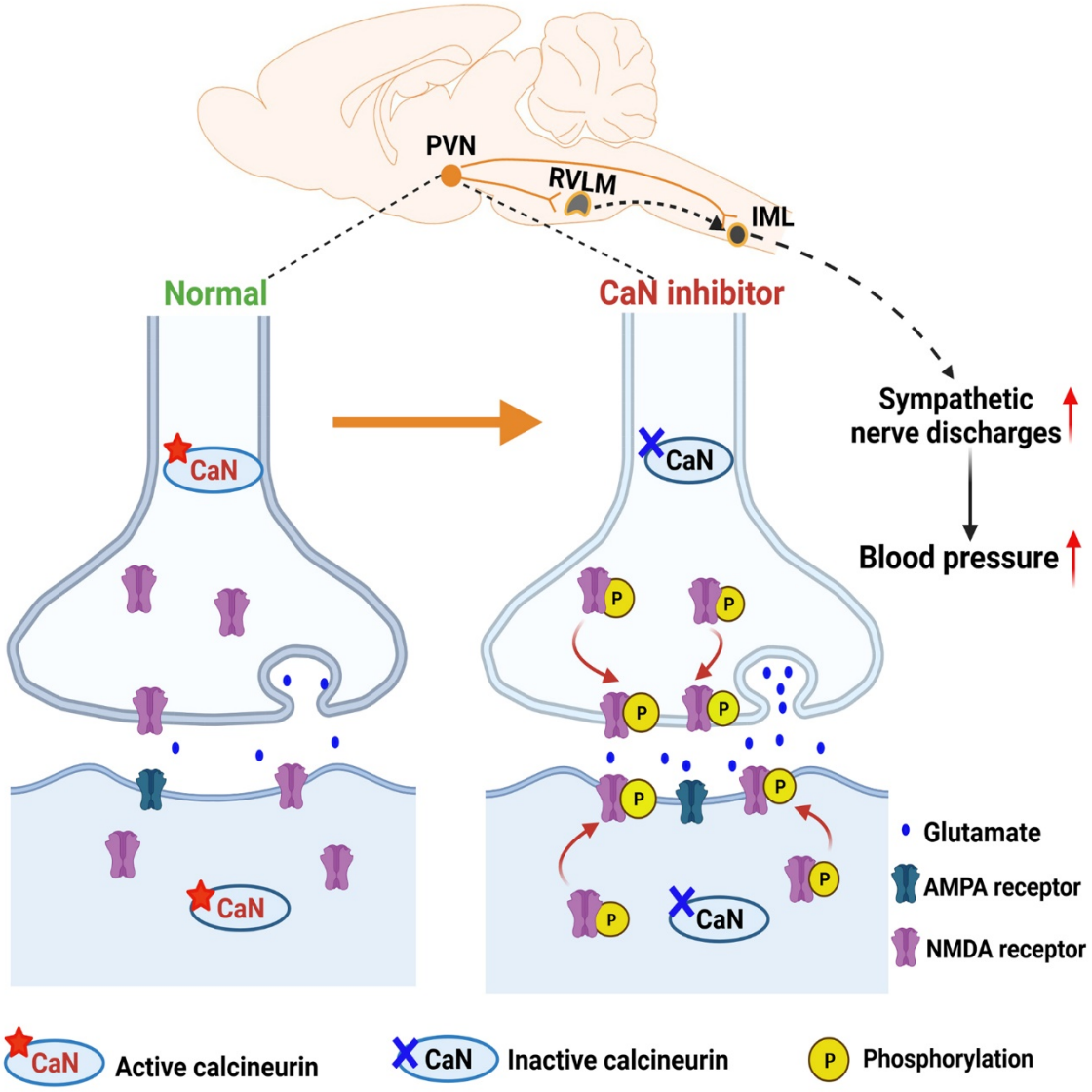

Figure S4. Schematic illustrating the major CNS sites and mechanisms of CIH. Under normal conditions, NMDARs are dephosphorylated by active calcineurin and stay away from the synaptic membrane in the PVN. Systemically administered calcineurin inhibitors can access to the PVN to diminish calcineurin activity, resulting in increased phosphorylation and synaptic trafficking of NMDARs. Consequently, augmented activity of presynaptic and postsynaptic NMDARs potentiates glutamatergic input to RVLM- and spinal IML-projecting PVN neurons, which constitutes an excitatory drive to increase sympathetic nerve discharges and vasomotor tone.

Table S1-1. Adjusted *p* values for MAP comparisons in Figure 1A.

Time / *p* values	MAP comparisons between FK506 and vehicle groups in light cycle	MAP comparisons between FK506 and vehicle groups in dark cycle	MAP vs. the baseline within FK506 group in light cycle	MAP vs. the baseline within FK506 group in dark cycle
Day 13	4.69e-04	2.23e-02	4.79e-02	1.73e-02
Day 14	1.77e-05	1.11e-02	3.51e-03	1.77e-02
Day 15	5.28e-05	8.59e-03	6.04e-03	6.35e-03
Day 16	8.43e-08	8.19e-04	5.17e-03	5.50e-03
Day 17	7.42e-09	1.63e-04	9.15e-03	5.47e-03
Day 18	1.08e-09	4.08e-06	7.32e-03	4.78e-03
Day 19	9.31e-10	3.24e-06	3.38e-03	1.70e-03
Day 20	8.26e-11	7.51e-07	4.64e-03	1.93e-03
Day 21	4.78e-08	6.93e-07	8.70e-04	1.00e-05
Day 22	2.18e-11	3.35e-07	9.05e-03	9.67e-03
Day 23	1.11e-11	3.02e-07	2.99e-03	6.81e-04
Day 24	2.50e-14	2.60e-07	2.24e-03	8.11e-04
Day 25	1.36e-08	1.13e-06	1.27e-03	5.17e-03
Day 26	1.06e-10	5.70e-07	2.21e-03	9.19e-03
Day 27	1.40e-10	4.86e-08	8.89e-04	4.91e-03
Day 28	2.23e-10	1.44e-07	5.03e-03	4.20e-04

Table S1-2. Adjusted *p* values for HR comparisons in Figure 1B.

Time / *p* values	HR comparisons between FK506 and vehicle groups in light cycle	HR comparisons between FK506 and vehicle groups in dark cycle	HR vs. the baseline within FK506 group in light cycle	HR vs. the baseline within FK506 group in dark cycle
Day 16	1.03e-01	2.43e-01	2.53e-02	1.01e-02
Day 17	1.30e-03	1.64e-04	5.77e-03	2.54e-04
Day 18	4.79e-03	1.60e-04	2.01e-03	1.00e-05
Day 19	5.35e-03	3.32e-03	1.13e-03	1.00e-05
Day 20	8.96e-03	3.79e-04	2.03e-03	1.20e-04
Day 21	2.60e-03	1.77e-04	3.03e-03	1.19e-04
Day 22	1.67e-03	5.23e-04	3.66e-03	1.20e-04
Day 23	7.54e-03	3.51e-04	9.51e-04	1.20e-04
Day 24	1.21e-03	5.51e-04	1.39e-03	1.20e-04
Day 25	2.11e-04	6.29e-05	1.25e-03	1.00e-05
Day 26	1.45e-03	3.76e-03	8.51e-04	1.20e-04
Day 27	1.41e-03	1.40e-03	1.00e-05	1.00e-05
Day 28	4.68e-03	1.70e-03	1.27e-03	1.20e-04

Table S2-1. Adjusted *p* values for MAP comparisons in light/dark cycle in Figure 8C.

Time / *p* values	MAP comparisons between the two groups in light cycle	MAP comparisons between the two groups in dark cycle	MAP vs. baseline within FK506 + memantine group in light cycle	MAP vs. baseline within FK506 + memantine group in dark cycle
Day 13	5.22e-01	3.91e-01	4.79e-02	1.73e-02
Day 14	1.41e-01	2.54e-01	3.51e-03	1.77e-02
Day 15	1.02e-01	2.19e-01	6.04e-03	6.35e-03
Day 16	1.26e-01	1.11e-01	5.17e-03	5.50e-03
Day 17	3.11e-02	4.99e-03	9.15e-03	5.47e-03
Day 18	3.24e-03	1.83e-03	7.32e-03	4.78e-03
Day 19	5.33e-04	1.22e-03	3.38e-03	1.70e-03
Day 20	8.83e-05	1.41e-03	4.64e-03	1.93e-03
Day 21	2.41e-03	3.45e-04	8.70e-04	1.00e-05
Day 22	1.51e-04	1.47e-04	9.05e-03	9.67e-03
Day 23	2.76e-04	5.26e-04	2.99e-03	6.81e-04
Day 24	1.57e-05	3.40e-04	2.24e-03	8.11e-04
Day 25	1.66e-07	1.76e-04	1.27e-03	5.17e-03
Day 26	2.79e-06	4.33e-05	2.21e-03	9.19e-03
Day 27	4.69e-06	2.44e-04	8.89e-04	4.91e-03
Day 28	3.46e-07	5.68e-05	5.03e-03	4.20e-04

Table S2-2. Adjusted *p* values for HR comparisons in light/dark cycle in Figure 8D.

Time / *p* values	HR comparisons between the two groups in light cycle	HR comparisons between the two groups in dark cycle	HR vs. baseline within FK506 + memantine group in light cycle	HR vs. baseline within FK506 + memantine group in dark cycle
Day 16	1.00e+00	1.00e+00	1.95e-02	6.84e-03
Day 17	1.48e-01	1.51e-01	5.73e-03	3.11e-03
Day 18	6.12e-02	1.32e-01	6.53e-04	2.94e-02
Day 19	3.00e-02	4.57e-02	1.07e-03	7.78e-04
Day 20	3.61e-02	2.43e-02	1.87e-03	1.72e-03
Day 21	2.16e-02	9.30e-03	3.08e-04	5.18e-04
Day 22	3.52e-02	1.04e-02	3.76e-03	1.32e-03
Day 23	9.97e-03	1.19e-02	7.77e-03	5.74e-04
Day 24	4.46e-03	3.03e-03	6.38e-04	5.67e-04
Day 25	5.33e-04	4.01e-03	4.51e-03	8.42e-04
Day 26	1.32e-03	1.39e-03	2.04e-04	1.20e-04
Day 27	1.12e-03	1.08e-03	9.89e-04	2.62e-03
Day 28	6.53e-04	8.77e-04	2.56e-03	5.25e-04

Table S3-1. Adjusted *p* values for SAP and DAP comparisons in light cycle in Figure S1A-B.

Time / *p* values	SAP comparisons between the two groups	SAP vs the baseline within FK506 group	DAP comparisons between the two groups	DAP vs the baseline within FK506 group
Day 13	8.83e-05	5.11e-03	1.70e-03	4.95e-03
Day 14	8.40e-07	3.44e-03	2.86e-03	4.56e-03
Day 15	4.74e-04	9.31e-03	4.91e-04	4.33e-03
Day 16	2.03e-07	2.63e-03	8.77e-06	1.06e-03
Day 17	1.04e-08	1.75e-03	1.92e-06	2.28e-03
Day 18	4.60e-08	2.15e-04	7.41e-08	2.47e-03
Day 19	2.32e-12	1.39e-03	7.88e-06	3.93e-03
Day 20	1.30e-13	5.20e-03	1.64e-06	3.06e-03
Day 21	4.50e-14	1.38e-03	2.52e-03	1.36e-03
Day 22	6.45e-12	1.07e-03	5.42e-08	3.86e-03
Day 23	8.30e-14	2.02e-03	1.88e-07	4.75e-03
Day 24	7.99e-13	2.67e-03	2.91e-11	1.87e-03
Day 25	4.20e-14	6.70e-04	7.17e-04	2.72e-03
Day 26	5.22e-13	9.80e-04	1.19e-06	5.60e-03
Day 27	1.00e-15	1.00e-05	4.87e-05	4.12e-03
Day 28	1.00e-15	1.81e-04	4.55e-05	3.71e-03

Table S3-2. Adjusted *p* values for SAP and DAP comparisons in dark cycle in Figure S1C-D.

Time / *p* values	SAP comparisons between the two groups	SAP vs the baseline within FK506 group	DAP comparisons between the two groups	DAP vs the baseline within FK506 group
Day 13	6.70e-04	3.05e-02	1.94e-01	3.70e-02
Day 14	2.73e-05	1.29e-02	2.18e-01	4.39e-02
Day 15	5.14e-04	4.91e-03	7.06e-02	2.43e-02
Day 16	4.60e-07	1.78e-02	5.26e-02	9.12e-03
Day 17	1.75e-10	3.21e-03	5.14e-02	1.54e-02
Day 18	3.16e-10	1.13e-03	9.14e-04	1.76e-02
Day 19	3.30e-14	6.79e-04	1.77e-02	6.32e-03
Day 20	1.00e-15	9.04e-04	3.68e-02	5.91e-03
Day 21	2.12e-13	5.06e-03	1.00e-03	1.00e-05
Day 22	4.93e-13	1.34e-03	3.67e-04	3.12e-02
Day 23	1.00e-15	7.67e-04	5.29e-03	2.44e-03
Day 24	2.00e-15	1.26e-03	1.26e-03	1.01e-03
Day 25	3.25e-13	2.26e-03	1.50e-03	1.62e-02
Day 26	5.00e-15	3.45e-03	2.13e-03	3.43e-02
Day 27	1.70e-14	2.67e-04	1.15e-04	2.65e-02
Day 28	2.34e-13	7.28e-03	1.81e-04	2.51e-04

Table S4-1. Adjusted *p* values for SAP and DAP comparisons in light cycle in Figure S3A-B.

Time / *p* values	SAP comparisons between the two groups	SAP vs the baseline within FK506 + memantine group	DAP comparisons between the two groups	DAP vs the baseline within FK506 + memantine group
Day 13	1.00e+00	3.74e-02	1.00e+00	6.47e-03
Day 14	1.00e+00	2.38e-02	2.54e-01	1.90e-04
Day 15	1.36e-01	1.71e-03	6.59e-01	3.56e-02
Day 16	9.97e-02	1.56e-03	2.24e-01	3.31e-02
Day 17	2.06e-01	6.77e-04	4.28e-03	5.22e-03
Day 18	2.21e-03	1.20e-04	2.45e-03	6.80e-03
Day 19	4.66e-03	2.99e-04	1.51e-03	2.63e-02
Day 20	8.35e-03	4.28e-04	8.35e-05	7.00e-03
Day 21	1.19e-02	1.00e-05	6.84e-03	2.61e-03
Day 22	7.20e-03	1.00e-05	1.98e-04	3.51e-03
Day 23	5.77e-03	1.20e-04	1.55e-03	5.83e-03
Day 24	3.47e-04	1.00e-05	3.81e-04	4.34e-02
Day 25	5.12e-05	1.00e-05	4.65e-06	1.13e-03
Day 26	1.52e-05	1.00e-05	6.87e-04	1.31e-03
Day 27	4.02e-06	1.52e-04	2.75e-03	4.61e-02
Day 28	2.27e-05	1.01e-04	4.36e-05	1.24e-03

Table S4-2. Adjusted *p* values for SAP and DAP comparisons in dark cycle in Figure S3C-D.

Time / *p* values	SAP comparisons between the two groups	SAP vs the baseline within FK506 + memantine group	DAP comparisons between the two groups	DAP vs the baseline within FK506 + memantine group
Day 13	1.00e+00	5.98e-03	1.96e-01	3.09e-02
Day 14	1.92e-01	1.04e-02	5.99e-01	1.95e-03
Day 15	2.34e-01	1.00e-05	2.50e-01	3.38e-02
Day 16	1.61e-01	2.50e-03	5.40e-01	1.20e-04
Day 17	1.58e-02	2.27e-02	4.71e-02	9.04e-04
Day 18	5.59e-04	1.00e-05	4.38e-02	1.20e-04
Day 19	2.04e-05	3.88e-04	1.96e-02	1.60e-04
Day 20	6.07e-05	1.05e-04	3.71e-02	1.15e-03
Day 21	1.38e-05	1.00e-05	3.64e-03	2.09e-03
Day 22	1.10e-04	3.83e-04	6.34e-03	1.35e-03
Day 23	1.22e-06	1.00e-05	2.58e-02	3.14e-04
Day 24	1.24e-06	1.78e-04	1.92e-02	1.52e-03
Day 25	6.64e-07	1.20e-04	4.40e-02	8.73e-03
Day 26	2.29e-09	1.96e-04	6.49e-03	5.00e-04
Day 27	1.30e-08	2.83e-04	1.66e-02	1.00e-05
Day 28	3.18e-07	1.20e-04	1.19e-02	3.19e-03